2.6 Supercooled Cloud Tunnel Studies on the Growth Conditions of Branched Planar Snow Crystals between −12°C and −17°C

Tsuneya Takahashi

Hokkaido Univ. of Education, Sapporo, 002-8502, Japan

1. INTRODUCTION

Snow crystals grow by vapor diffusion and play an important role in the formation of precipitation and related atmospheric processes. Of these, the planar types of branched crystals have the greatest variety of habit and are generally well-known as the representative shape of a snow crystal. But how does liquid-water content (LWC) and temperature affect the growth of branched planar snow crystals in clouds?

In the atmosphere, branched snow crystals grow as they fall through a supercooled droplet cloud. The airstream flowing past the crystal brings both vapor and droplets closer to the crystal, both of which can increase the mass and heat transfer. Thus, to understand the influence of this mass and heat transfer, one must grow the crystals in free fall. Laboratory experiments of free-falling, ice-crystal growth were done by Fukuta (1969), Ryan et al. (1974, 1976), Michaeli and Gallily (1976), and Song and Lamb (1994), but the growth times were all 4 min or less, meaning that branches did not develop sufficiently to distinguish the various subtypes. Much longer growth periods are required for a detailed study of branch development.

To this end, a vertical supercooled cloud tunnel was developed in which a single snow crystal could be freely suspended and continuously grown in front of the observer (Takahashi and Fukuta 1988; Takahashi et al. 1991; Fukuta and Takahashi 1999). The tunnel can simulate the process by which a snow crystal continuously grows while falling in a natural cloud. However, this previous study examined crystals in increments of about 0.5°C, and with an average temperature fluctuation of 0.4°C over 10 min, both of which are too coarse for the highly temperature-sensitive crystals, particularly in the branched planar regime. Moreover, the role of LWC had not been examined.

Here we use the vertical supercooled cloud tunnel with a finer temperature increment of 0.1°C to study the snow crystal growth process. We also address the fog effect from the supercooled droplets surrounding a snow crystal in a cloud by varying the LWC from 0.07 to 0.76 g m^{-3} over the entire branched planar regime.

2. EXPERIMENTS

The vertical supercooled cloud tunnel used here is the same as that in Takahashi et al. (1991). In the tunnel, a snow crystal can be suspended freely and grown in a vertical stream of artificially generated supercooled cloud by applying aerodynamical mechanisms for horizontal stability and by continuously adjusting the upward wind speed to match that of the (generally increasing) crystal fallspeed. The tunnel was set in a cold room where temperature could be more precisely controlled than that of the previous study. It was located at the Hokkaido University of Education in Sapporo, Japan, with an annual mean atmospheric pressure of about 1010 hPa.

Experiments were run for a snow crystal growth time of 10 min under isothermal and water-saturated conditions from −12 to −17°C with constant LWC values. The cloud temperature and the upward wind speed are measured by a thermistor and a hot-wire anemometer, respectively, and continuously monitored. The dewpoint, determined by evaporating the cloud, is also continuously monitored by a quartz dewpoint hygrometer. Then, the LWC is calculated from the air temperature and the dewpoint, assuming water saturation. The diameters of most droplets range from 4 to 10 µm, with an average diameter of approximately 8 µm: cloud droplet size distributions were measured by an impaction method. These parameters vary only slightly with changes in LWC. The initial crystal shapes were plate, thick plate, or column, with maximum dimension ranging from 5 to 20 µm and of about 10 µm on average. Runs having a maximum fluctuation in air temperature exceeding 0.2°C after the first minute of growth time are excluded. For fluctuations in LWC, the standard deviation is 0.067 g m^{-3} on average, with a maximum of 0.14 g m^{-3}. If riming became excessive, with the crystal collecting more than 120 cloud droplets, that LWC run was excluded. As the average drop size was about 14 µm in diameter (as manually measured on a photograph), the total mass of rimed droplets on a crystal should be less than 0.17 µg, a negligible contribution to the crystal mass (~4–8 µg). We similarly excluded crystals containing one or more spatial dendrites. However, between −15.0 and −15.5°C, spatial crystals developed so readily that it was nearly impossible to exclude all of them. Of those that remain in the analyses, their mass (e.g., the estimated 0.12 µg of the case at −15.0°C and 0.58 g m^{-3} in Fig. 4), have negligible contribution to the total crystal mass. In total, 167 cases were analyzed in this paper.

3. RESULTS AND DISCUSSION

3.a. crystal type

Figure 1 shows the variations of snow crystal type at two different LWCs with temperature. As the temperature decreases, the following forms occur: sector (P2a), broad-branch (P2b), stellar (P3a), and dendrite (P3b), then, with further cooling, the sequence reverses, reaching the sector form at about −16.3°C. At sufficiently high LWC (upper figures for LWCs between 0.37 and 0.58 g m^{-3}), the stellar and dendrite regimes change further to dendrite and fern (P3c) at −13.7 and −14.3°C, respectively; but at the other temperature, the crystal type is independent of LWC. Here, a sector has six wide sector-like branches. A broad branch has wide branches and parallel side faces in each branch and is intermediate between a sector and a stellar. A stellar has six long, narrow branches. A dendrite has side branches, and a fern has a high density of side branches. In particular, after 10-min of growth, a dendrite must have at least three crystal branches that each contain two or more sidebranches, whereas a fern must have at least three branches that each contain four or more sidebranches. The symbols in parentheses are from the new classification in Kikuchi et al. (2013).

The boundaries between these crystal types are shown as a variation of the Nakaya habit diagram in Fig. 2. The crystal habits are divided mainly by temperature, warm-to-cold into nine regions: sector above −12.5°C, then broad-branch to −13.0°C, then stellar, dendrite, and fern to −14.5°C; then the pattern reverses, with dendrite to −14.8°C, stellar to

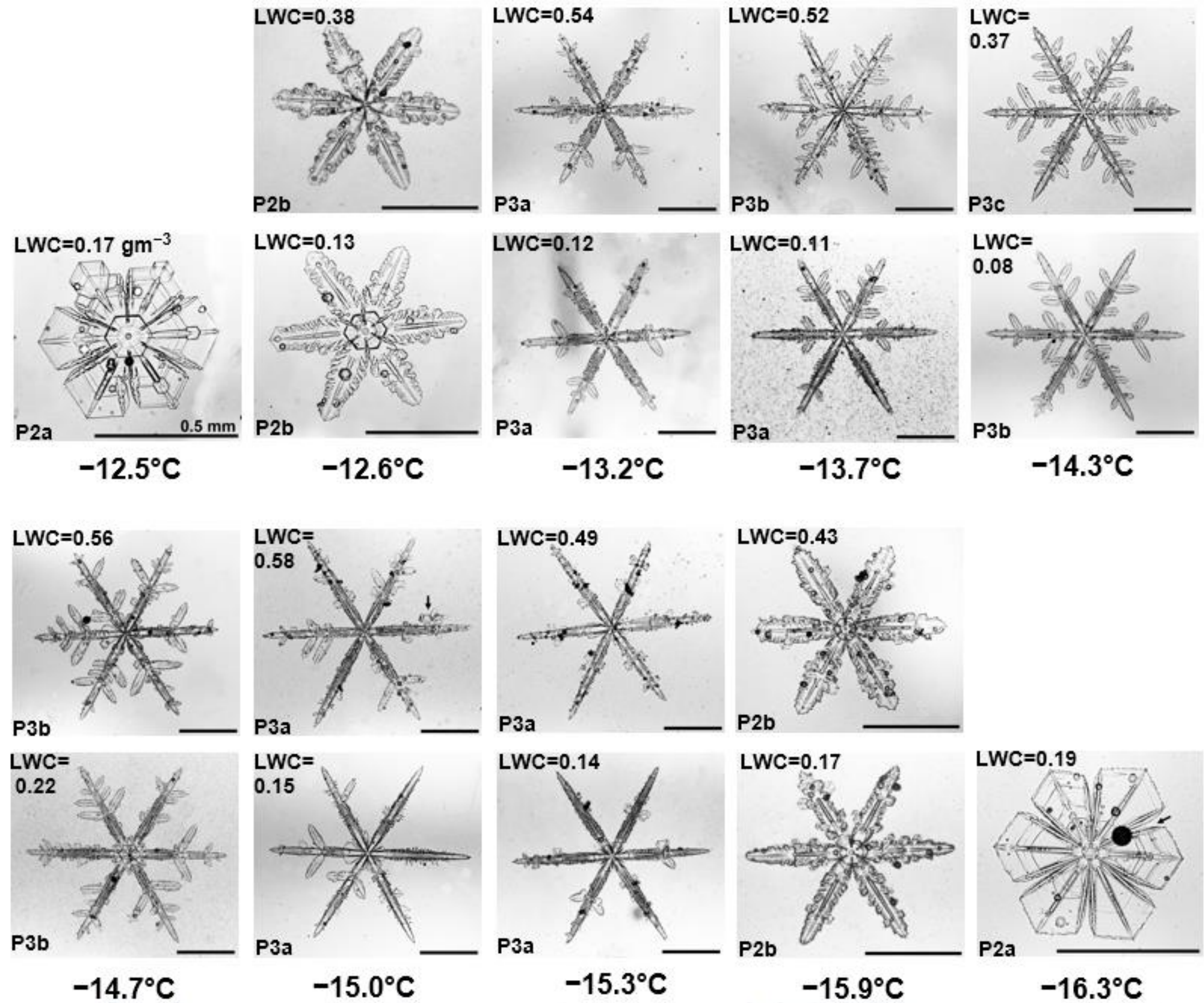

Fig. 1. Variations of crystal shape on temperature after 10 min of growth. At each temperature, a lower photo is for LWCs between 0.08 and 0.22 g m^{-3}, an upper one is for LWCs between 0.37 and 0.58 g m^{-3}. The upper and lower left of each crystal shows LWC (g m^{-3}) and the crystal type (see legend, Fig. 2). The arrow in the crystal at −15.0°C, 0.58 g m^{-3} marks a spatial dendrite that broke off the mother crystal. Black circles, such as that marked by an arrow at −16.3°C, are air bubbles in the oil that surrounds the crystals. Scale bar equals 0.5 mm in all images.

−15.7°C, broad-branch to −16.1°C, and finally sector. From −13.3 to −13.8°C, stellar changes to dendrite with LWC increase as well as with temperature decrease. From −13.8 to −14.5°C, dendrites coexist with ferns below a LWC of 0.25 g m^{-3}, but only ferns exist at higher LWC.

Sidebranch density is thought to be related to fluctuations in the growth conditions, suggested by Hallett and Knight (1994) and Nelson (2005). However, these models cannot explain why sidebranches formed at higher temperatures but not lower. A more detailed theoretical treatment thus appears necessary for understanding sidebranching in snow crystals.

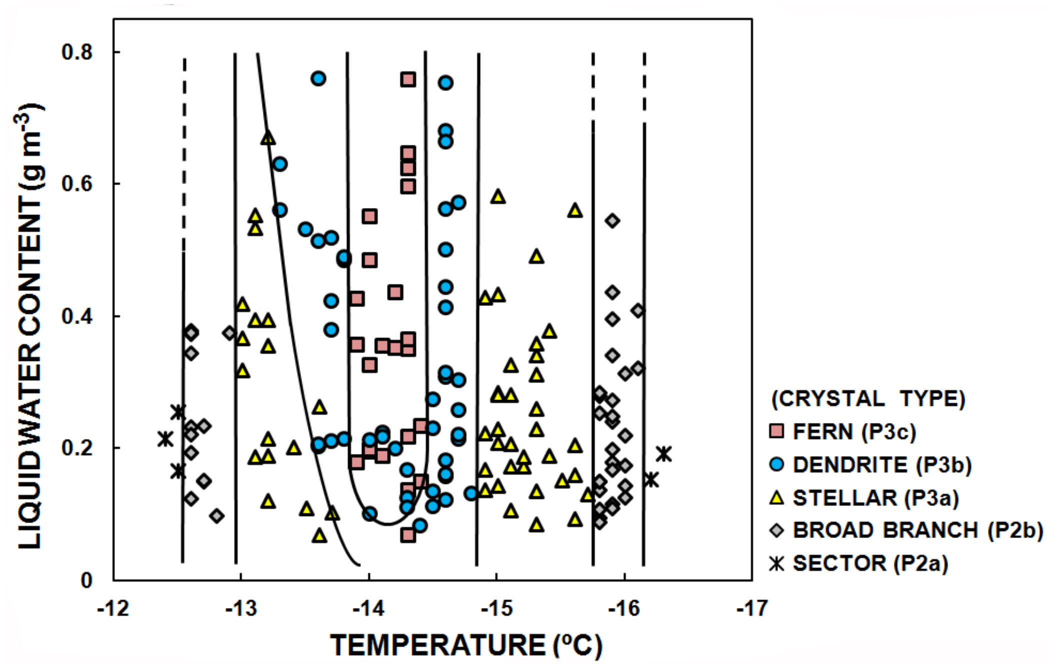

Fig. 2. Habit, temperature, and LWC of each crystal analyzed. The crystals were grown for 10 min.

3.b. crystal diameter, mass, apparent crystal density with temperature

Figure 3 shows the variation of crystal diameter, which is the crystal length along the a-axis from branch-tip to opposite branch-tip, with temperature. As the temperature decreases, the diameter rapidly increases from −12.4 to −13.3°C, where the crystal shapes change from sector to broad-branch to stellar. The rate of increase slows below −13.3°C, about where the sidebranches appear, and becomes a small depression near −14°C, where the sidebranch-rich fern habit appears. At −14.9°C, soon after the sidebranches vanish, the growth rate peaks. This behavior suggests that the sidebranches are depleting the air of vapor, particularly vapor that would otherwise contribute to the branch tips and increase the crystal diameter. Upon further cooling (−15.3 to −16.3°C), the diameter rapidly decreases, where the reverse pattern of stellar to broad-branch to sector occurs.

The trend in crystal mass with temperature is similar to that for crystal diameter. As the crystal shape changes from a sector at −12.4°C to a broad-branch, then to a stellar at −13.3°C, the mass rapidly increases, as shown in Fig. 4. As temperature decreases further, the mass increases more slowly. The slowdown starting just below −13.3°C is similar to that for diameter, but not as pronounced. The reason is likely due to the sidebranches depleting vapor that would otherwise deposit on the tip, but in this case, the mass increase of the sidebranches also contributes to the crystal mass. As with the diameter, the peak is at −14.9°C, where stellars form. At lower temperatures, particularly below −15.3°C, the mass decreases rapidly. The mass data shows more spread for a given temperature, with the higher LWC data (in red dashed) generally higher than that for the lower LWC (in blue solid). Thus, unlike the case with crystal diameter, the crystal mass increases with an increase of LWC.

Concerning the sharp rate peaks, the

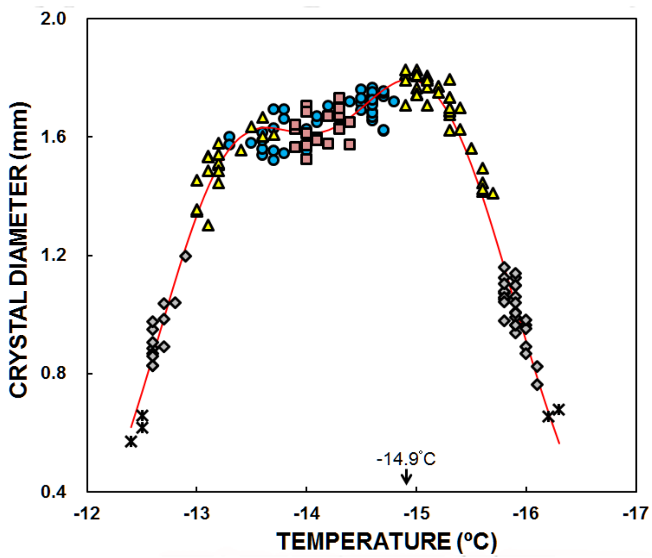

Fig. 3. Crystal diameter after 10 min of growth with temperature. The data and symbols are the same as those in Fig. 2. Fitting curve is for all LWCs. The arrow marks the maximum.

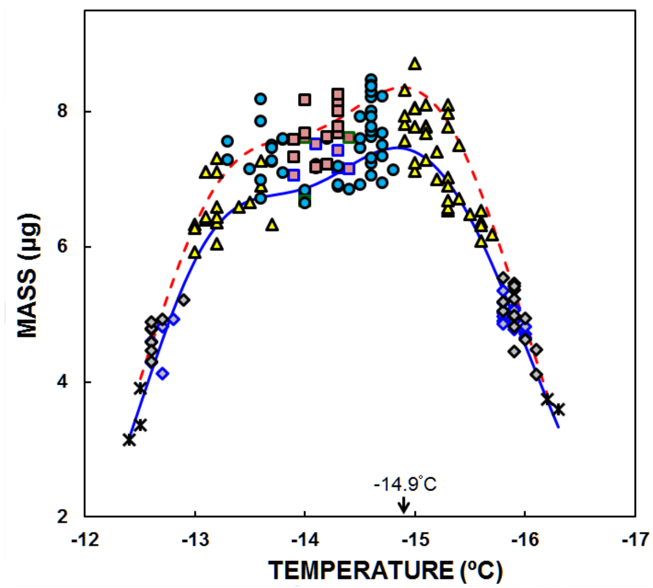

Fig. 4. Crystal mass after 10 min of growth. Data and symbols are the same as those in Fig. 3. Blue solid fitting curve is for LWCs between 0.07 and 0.2 g m^{-3}, red dashed curve is for LWCs between 0.35 and 0.76 g m^{-3}. The arrow marks the maximum.

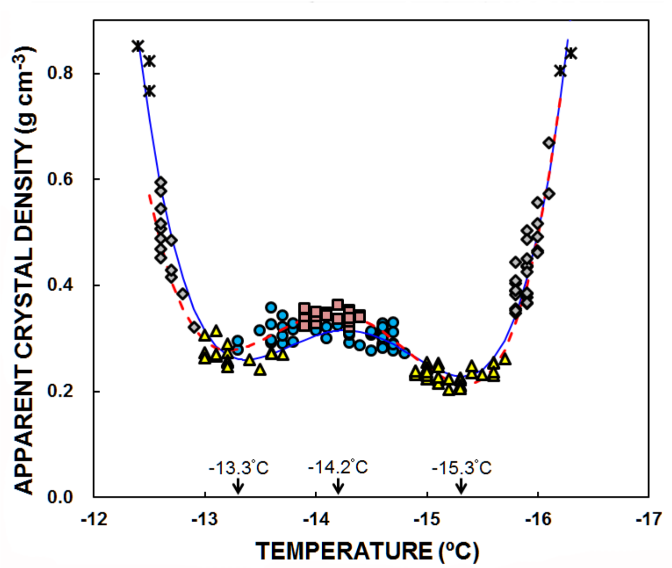

Fig. 5. Apparent crystal density after 10 min of growth. Data, symbols, and fitting curves are the same as those in Fig. 3. Arrows mark the minima and local maximum.

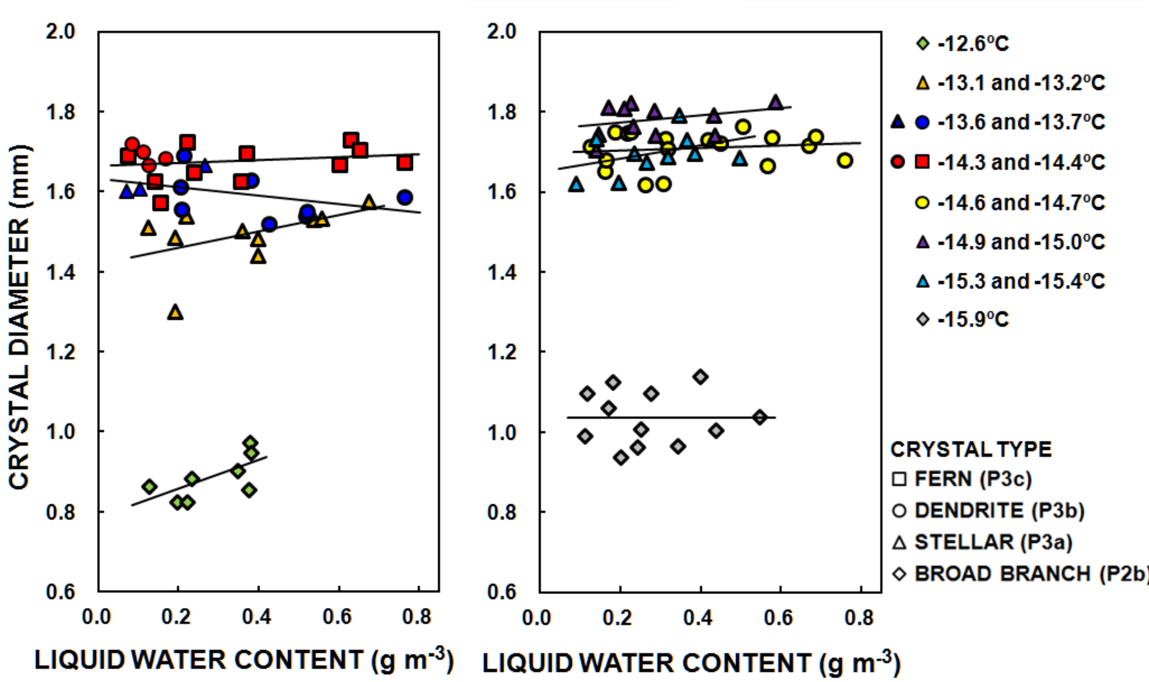

Fig. 6. Crystal diameter after 10 min of growth versus LWC at various temperatures. The solid lines are straight-line fits.

environmental and bulk-ice parameters that influence the mass growth rate (e.g., supersaturation and latent heat of deposition) vary only slightly over the present temperature range, and thus cannot explain these large changes. For example, in Maxwell's growth law with the capacitance analogy, if the shape factor, the fog factor, and the ventilation factor are held fixed, the growth rate would peak at −14.25°C at 1000 hPa (e.g., Byers, 1965). Moreover, the variation in growth rate between −12.4 and −16.3°C would be predicted to be less than 1.4% of the peak value. Both predictions fail to explain the data. Thus, according the law, the measured variation in mass growth rate must be due to changes in the above three factors. The change in the shape factor is due to the change in crystal diameter. The diameter, in turn, is strongly influenced by surface processes, which are ultimately the cause of the growth-rate peaks.

The 'openness' of the ice structure is roughly the ratio of the basal plane area to the area of a circumscribed hexagon. This quantity, when multiplied by the density of ice, is called here the apparent density. The density decreases from −12.4 to −13.3°C as the crystal shape changes from sector to broad-branch to stellar (Fig. 5). The reverse trend occurs from −15.3 to −16.3°C. In between, the density shows a local maximum at −14.2°C where the sidebranch-dense ferns grow. The highest density of sidebranches does not occur at the maximum growth rate. On either side, local minima occur at −13.3 and −15.3°C, both where stellars grow. The relatively large spread in density values between about −13.5 and −14.5°C is due to the crystals developing more sidebranches at higher LWC values. This spread does not occur near −15°C because the crystals have no sidebranches.

3.c. crystal diameter and mass vs LWC

Figure 6 shows the changes in crystal diameter with changes in the liquid water

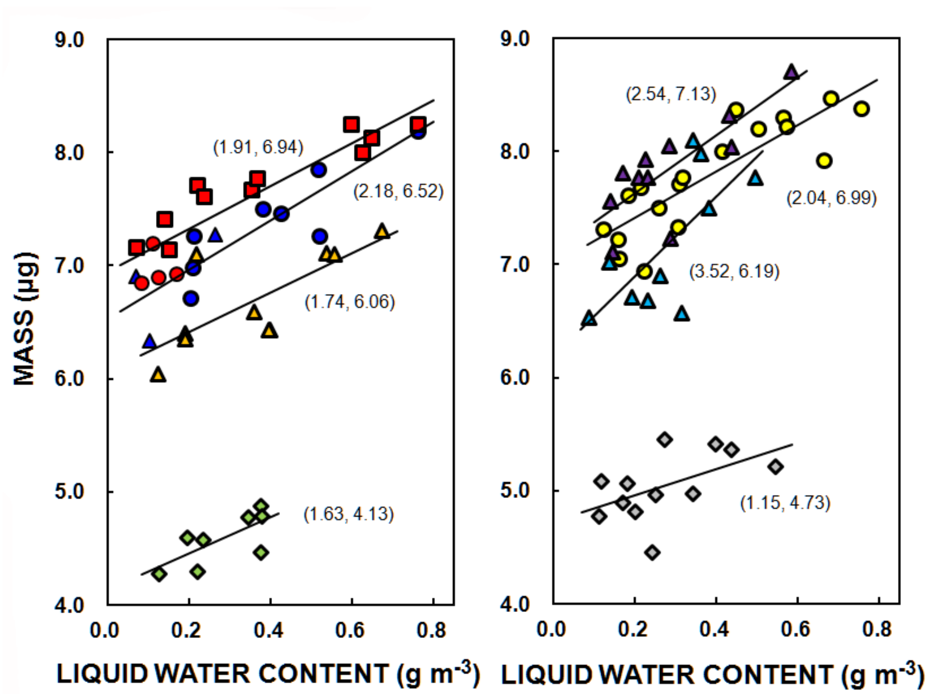

Fig. 7. Crystal mass after 10 min of growth versus LWC at various temperatures. Data and symbols are the same as those in Fig. 6. Numbers in parenthesis give the slope, and vertical intercept for each regression line. The correlation coefficients vary from 0.72 to 0.91 except the bottom right line, for which it is 0.53.

content at various temperatures. In contrast to the temperature trend, the diameter appears essentially independent of liquid water content.

The dependence of mass on LWC at several fixed temperatures is shown in Fig. 7, which indicates that the LWC changes cause the spread in mass values. Contrary to the diameter, the higher mass growth rate is most likely due to the larger local gradients of vapor density and temperature where the droplets closely approach the crystal. The trend in mass increase was consistent with the theoretical fog factor from Marshall and Langleben (1954).

The present results show that the apparent crystal density increases with an increase in LWC due to the growth of sidebranches between about −13.5 and −14.5°C. But at higher and lower temperatures, the increase in LWC hardly affects the density, meaning that the LWC increase does not produce more sidebranches, as observed. Since the diameter of the snow crystals is independent of LWC, but the mass increases with LWC, it follows that the mass increase at those warmer and lower temperatures must arise from an increase in crystal thickness. The cloud droplets, therefore, contribute to the development of sidebranches and probably also an increase in crystal (or branch) thickness. The possibility of the latter was pointed out by Nelson (2005) with a simple analysis indicating that a relatively large fraction of the water-vapor mass is uptaken on branch backsides (i.e., underside of the major level), which face the onrushing droplets when the crystal is in the stable fall orientation.

4. CONCLUSIONS

To study branched snow crystal growth in a cloud, a vertical wind tunnel studies were done. The main findings are as follows:

1) The crystal habits were dependent with temperature, with habit regimes roughly symmetric about the fern regime near −14.2°C. Away from this temperature were dendrites, then stellars, then broad-branch types, and then sectors.
2) Stellars transformed to dendrites between −13.3 and −13.8°C and dendrites transformed to ferns between −13.8 and −14.5°C. For the other temperatures, the crystal type was independent of LWC.
3) The maximum mass uptake and diameter both occurred at −14.9°C.
4) The apparent crystal density varies with temperature: the local maximum was at −14.2°C for ferns, and two local minima were near −13.3 and −15.3°C for stellars.
5) An increase in LWC produced an increase in the crystal mass.
6) LWC did not affect the crystal diameter.
7) The cloud droplets contribute not only to the development of sidebranches and probably but also an increase in crystal (or branch) thickness.

References

Byers, H. R., 1965: *Elements of Cloud Physics*. University of Chicago Press, 191 pp.

Fukuta, N., 1969: Experimental studies on the growth of small ice crystals. *J. Atmos. Sci.*, **26**, 522–531.

Fukuta, N. and T. Takahashi, 1999: The growth of atmospheric ice crystals: A summary of findings in vertical supercooled cloud tunnel studies. *J. Atmos. Sci.*, **56**, 1963–1979.

Hallett, J., and C. Knight, 1994: On the symmetry of snow dendrites. *Atmospheric Research*, **32**, 1–11.

Kikuchi, K, T. Kameda, K. Higuchi, A. Yama shita and working group members for new classification of snow crystals, 2013: A global classification of snow crystals, ice crystals, and solid precipitation based on observations from middle latitudes to polar regions. *Atmospheric Research*, **132–133**, 460–472.

Marshall, J. S., and M. P. Langleben, 1954: A theory of snow-crystal habit and growth. *J. Meteor.*, **11**, 104–120.

Michaeli, G. and I. Gallily, 1976: Growth rates of freely falling ice crystals. *Nature*, **259**, 110.

Nelson, J., 2005: Branch growth and side branching in snow crystals. *Crystal Growth & Design,* **5**, 1509–1525.

Ryan, B. F., E. R. Wishart, and E. W. Holroyd, 1974: The densities and growth rates of ice crystals between −5°C and −9°C. *J. Atmos. Sci.*, *31*, 2136–2141.

___, ___, and D. E. Shaw, 1976: The growth rates and densities of ice crystals between −3°C and −21°C. *J. Atmos. Sci.*, **33**, 842–850.

Song, N., and D. Lamb, 1994: Experimental investigations of ice in supercooled clouds. Part I: System description and growth of ice by vapor deposition. *J. Atmos. Sci.*, **51**, 91–103.

Takahashi, T., and N. Fukuta, 1988: Super cooled cloud tunnel studies on the growth of snow crystals between −4 and −20°C. *J. Meteor. Soc. Japan*, **66**, 841–855.

Takahashi, T., T. Endoh, G. Wakahama and N. Fukuta, 1991: Vapor diffusional growth of free-falling snow crystals between −3 and −23°C. *J. Meteor. Soc. Japan*, **69**, 15–30.

[For details, please refer to Takahashi (accepted in *J. Atmos. Sci.*).]